

6
4
7

V393
.R46

469

MIT LIBRARIES



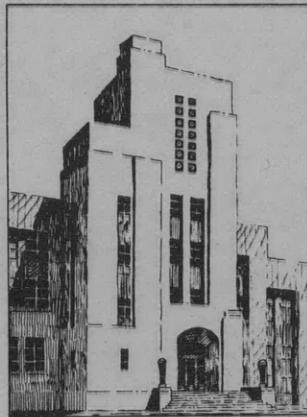
3 9080 02754 0787

THE DAVID W. TAYLOR MODEL BASIN

UNITED STATES NAVY

A CAVITATION METHOD FOR THE DEVELOPMENT OF FORMS
HAVING SPECIFIED CRITICAL CAVITATION NUMBERS

BY P. EISENBERG



~~CONFIDENTIAL~~

SEPTEMBER 1947

27

~~REPORT 6-14~~

Report 647

REPORT G-14

A CAVITATION METHOD FOR THE DEVELOPMENT OF FORMS
HAVING SPECIFIED CRITICAL CAVITATION NUMBERS

BY P. EISENBERG

SEPTEMBER 1947

CONFIDENTIAL

“This document contains information affecting the national security of the United States within the meaning of the Espionage Act, 50 U.S.C., 31 and 32, as amended. Its transmission or the revelation of its contents in any manner to an unauthorized person is prohibited by law.”

U.S. Navy Regulations, 1920, Art. 76(11).

A CAVITATION METHOD FOR THE DEVELOPMENT OF FORMS HAVING SPECIFIED CRITICAL CAVITATION NUMBERS

INTRODUCTION

During World War II, H. Reichardt, an assistant of L. Prandtl at Gottingen, Germany, developed an experimental method of designing body shapes for operation in air at speeds where compressibility effects become important. This method consists of determining surfaces having approximately constant pressure characteristics by photographing the shape of a cavitation bubble which is allowed to develop behind an obstacle in a stream. In Reference (1)*, it was proposed that the same technique might be used for developing shapes having any specified critical cavitation number. Specifically, the method was proposed for use in the design of hull shapes for high-speed torpedoes.

Experiments have been made to investigate the validity of the proposed method and to obtain data for correlation purposes. Cavitation bubbles induced behind a hemisphere, a half-ellipsoid, a truncated ogive, and discs of two sizes have been photographed at various values of the cavitation parameter. Data have also been gathered on the pressure distributions within cavitation bubbles and on the drag of the various head shapes when cavitating.

From measurements of photographs of the bubbles, a model has been constructed and the pressure distribution measured on the solid body of revolution obtained. It is the purpose of this report to present the results of the correlation between cavitation bubble and solid model constructed to the shape of the bubble. The results of the other investigations made in connection with this problem will be the subject of subsequent reports.

THEORY OF THE CAVITATION METHOD

Since the inception of cavitation on a solid body occurs at the point of minimum pressure*, the problem of

* Numbers in parentheses indicate references on the last page of this report.

** On blunt bodies and bodies having steeply rising pressure gradients, cavitation may occur in the vortices induced in the zone of separation of flow before it occurs at the point of minimum pressure on the body itself. This discussion is concerned only with the pressures on the body.

designing for specified critical cavitation* numbers is one of predetermining the minimum pressure coefficient for the body. In the case of a solid body, the Bernoulli equation written between a point in the free stream and the point of minimum pressure on the body is

$$P + \frac{1}{2} \rho V_0^2 = P_{min} + \frac{1}{2} \rho v^2 \quad [1]$$

where P is the pressure in the free stream,
 ρ is the mass density of the fluid,
 V₀ is the velocity of the free stream,
 P_{min} is the minimum pressure on the body and
 v is the velocity of the fluid at the point of minimum pressure on the body.

The pressure coefficient is then given by

$$\frac{\Delta P_{min}}{q} = \frac{P_{min} - P}{\frac{1}{2} \rho V_0^2} = 1 - \left(\frac{v}{V_0}\right)^2 \quad [2]$$

where q = $\frac{1}{2} \rho V_0^2$. At the inception of cavitation P_{min} approaches very closely the vapor pressure of the fluid.

For a cavitation bubble formed behind an elementary obstacle in the stream, such as a disc, the Bernoulli equation may be written as

$$P + \frac{1}{2} \rho V_0^2 = P_B + \frac{1}{2} \rho v_B^2 \quad [3]$$

where p_B is the pressure at the interface of the bubble and the fluid, and v_B is the velocity of the fluid at this interface. The cavitation parameter is then defined by

$$\sigma_c = \frac{P - P_B}{\frac{1}{2} \rho V_0^2} = \left(\frac{v_B}{V_0}\right)^2 - 1 \quad [4]$$

Since the cavitation bubble is, presumably, a constant pressure surface, the value of p_B, in absolute units, may be taken anywhere along the bubble**. Furthermore, the interface of the fluid and the cavitation bubble must be a stream line since there is no cross flow through this surface.

* The critical cavitation number is defined as the value of the cavitation parameter at which cavitation just begins.

** This assumption is not precise as will be shown in the subsequent discussion.

If, then, the cavity space is filled with a solid material preserving the shape of the bounding streamline, the pressure conditions along the boundary should be unchanged. (In an actual case, the effects of the reentrant jet at the end of the bubble and of the unstable bubble wake must be considered; these effects are discussed in the following sections.) In developing shapes from cavitation bubbles, then, the minimum pressure coefficient for the solid becomes the negative of the cavitation number at which the bubble was formed, or

$$\frac{\Delta P_{min}}{\rho} = -\sigma_c.$$

Furthermore, since cavitation ordinarily begins on the body at the value of the minimum pressure coefficient with p_{min} equal to the vapor pressure of the fluid, the critical cavitation number for this body is also given by σ_c .

EXPERIMENTAL PROCEDURES IN USING THE CAVITATION METHOD

In the actual design of bodies having specified critical cavitation numbers, the desired volume, the length-diameter ratio, and the head shape (which may be of importance for such problems as wave-making resistance) govern the selection of the elementary obstacle that is used in the experiments. For example, the body shape desired from bubbles formed behind discs have larger length-diameter ratios than those derived from hemispheres or semiellipsoids at the same cavitation number.

For the present investigations, only bodies of revolution were of interest for immediate application, so that all the elementary forms were of circular cross-section in the plane perpendicular to the stream. The flow direction was always parallel to the axis of symmetry of the obstacle. In practical applications, where the derived body will at times assume angles of pitch or yaw with the stream direction, it will be necessary to form the cavitation bubble at some number less than that required for straight running only. Proper selection of the test cavitation number will obviate the possibilities of cavitation due to the lowering of the minimum pressure coefficient when the body is at an angle of attack.

The experiments discussed herein were conducted in the 24-Inch Variable-Pressure Water Tunnel at the David Taylor Model Basin. The elementary heads were supported in the free tunnel jet at the end of a hollow tube, which in turn was secured to a hollow shaft downstream from the head. Pressure

taps in the hollow tube were placed $3/4$ inch behind the head and communicated with an absolute mercury manometer outside of the tunnel. The heads were $1\frac{1}{2}$ inches in diameter except for one disc model which was 0.989 inch in diameter. The two sizes of discs were used in an attempt to investigate the effects of scale. However, no scale effects were noted, but the range of Reynolds numbers was not sufficiently wide for conclusive data in this respect.

A range of cavitation numbers was obtained by varying the speed of flow and by varying the absolute pressure on the surface of the tunnel jet. The air content of the water and the temperature were allowed to vary at will. These variables were measured for each bubble obtained, and measurements were taken of the pressure within the bubble itself. At the same time, photographs were taken of the bubbles.

RESULTS OF THE CAVITATION TESTS WITH THE SMALL DISC MODEL

Since it is the purpose of this paper to present only the results of the first correlation obtained between cavitation bubble and corresponding solid, only the work on the small disc model on which these studies were conducted will be discussed. Additional studies (including the other head shapes) which have been completed or are underway will be reported in the near future.

It was found from the various measurements taken that, at least for the range of Reynolds numbers used on the experiments, the shape of the bubbles depends only on the shape of the elementary form and on the cavitation number. The German investigations mention no dependence on Reynolds number. However, their models were all sharp-edged so that flow separation was fixed at all Reynolds numbers. In the present experiments, flow separation was not fixed, even on the disc model which had a finite thickness. These effects are the subject of additional investigations now underway.

In no case in the present experiments was the measured pressure within the cavitation bubble found to be equal to the vapor pressure of the fluid. However, with a fairly high air content in the water, the pressure is probably very nearly the sum of the partial pressures of the

vapor and the gases which enter the bubble. Since the bubbles were fairly large (as much as 15 inches long in some cases), there was easily time enough for dissolved gases to enter the bubble.

Certain effects (to be described in more detail in forthcoming reports) led to subsequent surveys of the pressure distribution along the supporting tube in the interior of the bubble. As expected, it was found that there is a sizeable variation of the pressure within the bubble. In some cases, this variation was as much as 15 per cent between the highest pressure just behind the head and the lowest pressure which occurs over the major part of the bubble along its length. The pressure also rises near the end of the bubble, but for the present discussion, this fact is of little interest. Fortunately, the pressures measured in the bubbles when making the photographs were taken far enough behind the head so that they actually gave the maximum cavitation number for the bubble. Whether the same variations occur along the bubble surface remains to be investigated.

The photograph of the bubble formed behind the disc at cavitation number 0.255 is shown in Figure 1. This is an exposure of one or two seconds. To be sure that the time exposure did not obscure the actual action of the bubble, photographs were also taken at 1/30000 second. In Figure 2 is shown the same bubble as in Figure 1 but taken at the higher speed.

It is seen in Figures 1 and 2 that the bubble separates from the disc at some distance behind the leading edge and appears to leave at an angle of 90 degrees. Since this phenomenon is shown in both the low- and high-speed photographs, which were taken under different lighting conditions, the effect is believed to be real. The separation of the bubble at what appears to be a finite angle with the surface of the model is also present in the case of all the other models tested. Whether this is an effect of viscosity or is actually a possible flow configuration in which there is a reversal of curvature at separation, as has been shown for potential flow in the two-dimensional case (2), is being investigated.

In spite of the unstable bubble surface and the turbulent wake with its reentrant jet (as evidenced by the pressure distribution within the bubble), it was thought that the temporal average of the surface shown in Figure 1

could still be used for body shapes. As a result, a model was constructed to the shape of the bubble formed behind a disc at cavitation number 0.116.

PREPARATION OF CAVITATION MODEL D-116

For the first correlation model, the bubble obtained at the lowest cavitation number measured for the disc model was chosen. This bubble, with $C_v = 0.116$, is shown in Figure 3 and was designated "Cavitation Model D-116". It is seen that only about three-quarters of the bubble is clearly defined. To obtain coordinates, the photographs were enlarged until the maximum diameter was approximately 5 inches on the enlargement. The edge of the bubble was then drawn on the enlargement as far back from the head as could be done with any degree of accuracy. The after end of the bubble was faired by eye. The strong distortions on the actual surface precludes a sharp bubble outline on the photograph and leads to uncertainties in determining the shape of the surface so that after once drawing this line, it was never adjusted despite the temptations caused by the shading which appears after a black line is drawn on the photograph.

The problem of "closing" the bubble to form the solid body will depend upon the conditions for which the design is to be used. In any case, if the slopes and curvatures are maintained at the point at which the bubble disappears, or to which data is taken, any afterbody shape should be suitable. Since the afterbody will be in what was the wake of the bubble, it will not materially affect the pressure distribution on the part of the surface determined by the bubble. In general, the afterbodies will give a longer form than the original bubble with the result that the pressure distribution will be more favorable than for a body built with the abrupt afterbody of the actual bubble. The selection of the shape of the afterbody will be of importance in terms of its effects on the drag of the body as influenced by the rising pressure gradients on the afterbody.

For the present investigation, the slopes and curvatures were held, and the length-diameter ratio for the solid fixed at approximately 5. An equation, polynomial in form but with a square-root term to take account of the slope at the point of the bubble, was fitted to the experimental curve in order to insure continuity of the surface of the final model. This model, as prepared for the pressure distribution test,

is shown in Figure 4. The offsets of the model and the points measured from the photograph of the bubble are shown on Figure 5.

CORRELATION OF THE PRESSURE DISTRIBUTION ON CAVITATION MODEL D-116 WITH ITS PARENT BUBBLE FORM

Because of rather large pressure gradients in the jet of the 24-inch water tunnel, the model of the bubble was tested in the same position and with the same downstream conditions as for the bubble in order to minimize errors due to uncertainties in the boundary conditions. The tests were made over a fairly narrow range of Reynolds numbers varying from 1.8×10^6 to 4.7×10^6 , but this is probably high enough so that scale effects on the pressure distribution, at least, are negligible.

The results of the measurements are shown in Figure 6. Except for the peak value of $A_p = 0.14$ at the point where the curvature of the model surface is very high, the nearly constant average value of $A_p = -0.114$ is in excellent agreement with the "design" value of -0.116 . The peak value of -0.14 is probably due to inaccuracies in determining the coordinates of the bubble. It is easily seen that an extremely small change in the curvature of the model at this point will reduce the absolute value at this point considerably. Since, for most practical purposes, the bubbles will be developed behind heads which do not induce such high curvatures, errors in removing coordinates of the bubbles will not be as serious as in this case. In view of the many variables in the problem and the factors of non-constant bubble pressure and unstable bubble surface found during these tests, the results are extremely promising. Furthermore, from the standpoint of drag, the fact that adverse pressure gradients occur only near the end of the model indicates that forms developed in this manner will have lower drag than forms of the same critical cavitation number but less favorable pressure distributions. Such pressure distributions are characteristic of the low-drag laminar flow forms.

CONCLUDING REMARKS

Although the cavitation method proposed for use in developing bodies having specified critical cavitation numbers has been demonstrated to be a valid one, the problems,

which arose for the first time during these tests, require more thorough investigation before adopting the method as a standard technique. Apparently, the two most important effects to be investigated are:

1. the effect of the pressure distribution within the bubble on the pressure distribution along the surface of the bubble and, consequently on its shape; and

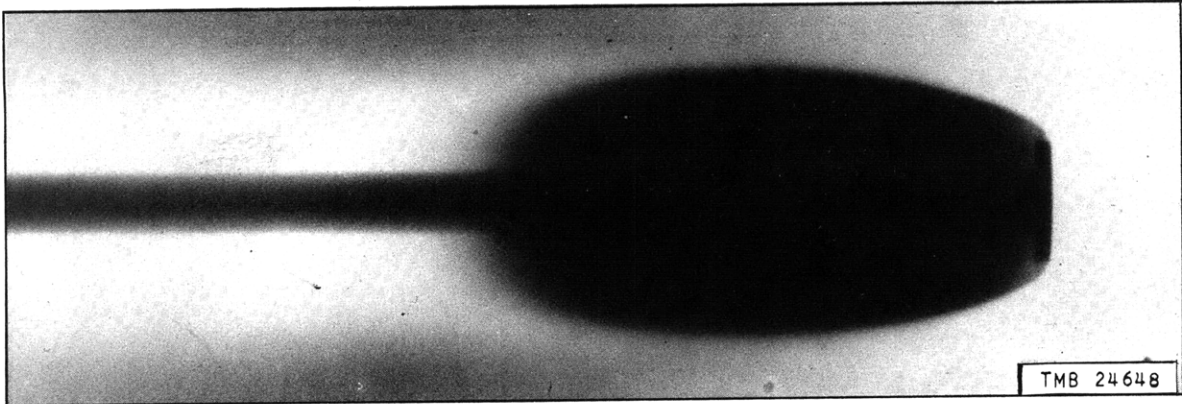
2. the nature of the phenomenon which causes the surface of the cavitation bubble to leave the elementary form at what appears to be a finite angle.

In connection with torpedo designs which require cylindrical middle bodies, the effects of inserting such a portion into a form developed by the proposed method require investigation. Although such a procedure may have undesirable effects on the drag characteristics of the form, the critical cavitation number may not be greatly affected.

REFERENCES

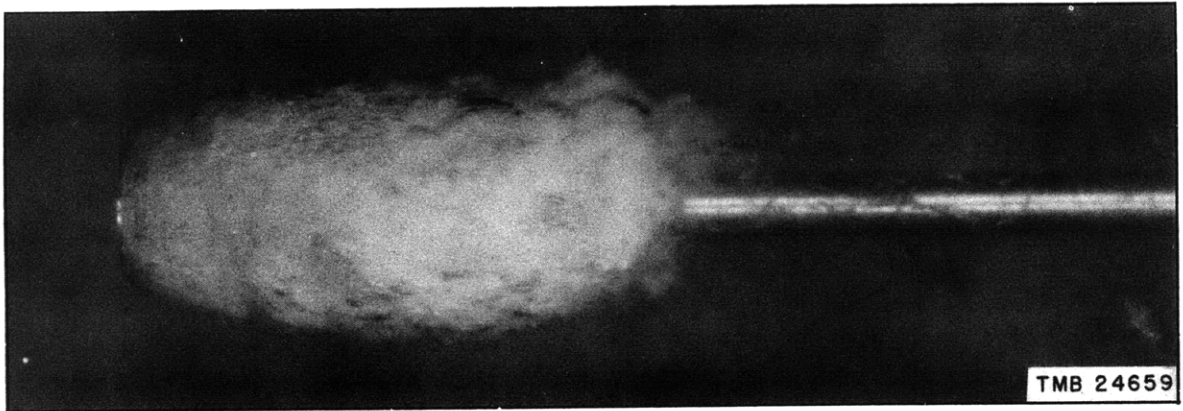
- (1) "Proposed Program of Research Leading to the Design of a High-Speed Submarine-Torpedo Hull, TMB Research E252-1", by P. Eisenberg, CONF, April 1947 (Enclosure (A) to TMB CONF ltr C-S75-1 of 9 May 1947 to BuOrd (Re-6)).

- (2) "Hydrodynamic Researches" by G. Kreisel, British Intelligence Objectives Subcommittee Report No. 108, London, 1945.



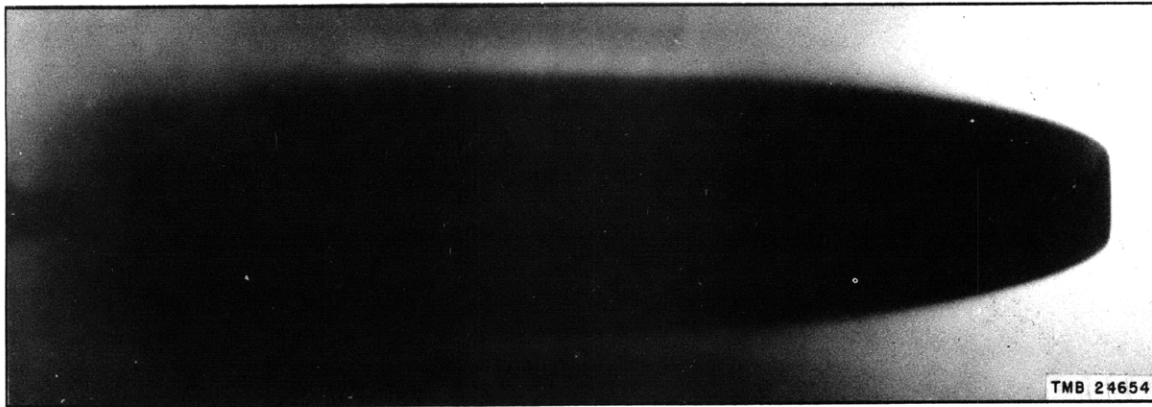
TMB 24648

Figure 1 - Time Exposure of the Cavitation Bubble Formed Behind
a Disc at $\sigma_0 = 0.255$



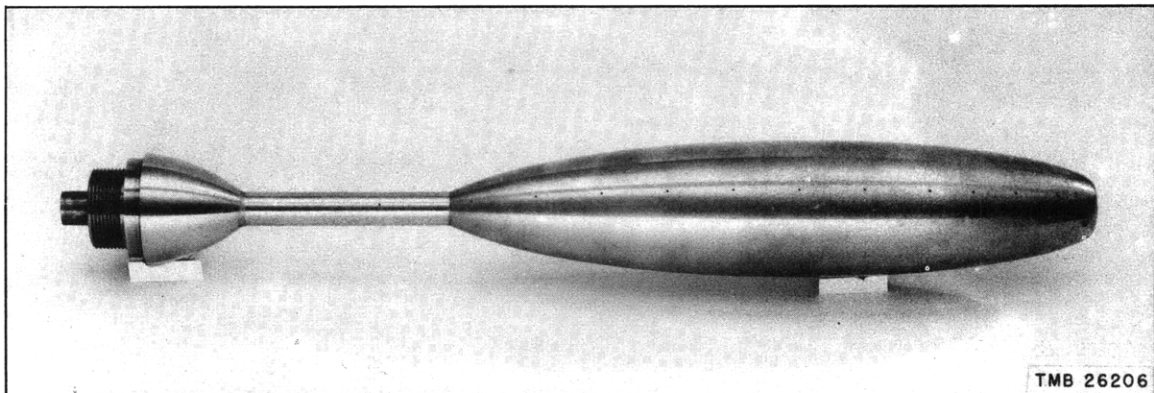
TMB 24659

Figure 2 - Photograph of the Bubble Shown in Figure 1 Taken
at An Exposure Time of $1/30,000$ second



TMB 24654

Figure 3 - Time Exposure of the Cavitation Bubble Formed Behind
a Disc at $\sigma_0 = 0.116$

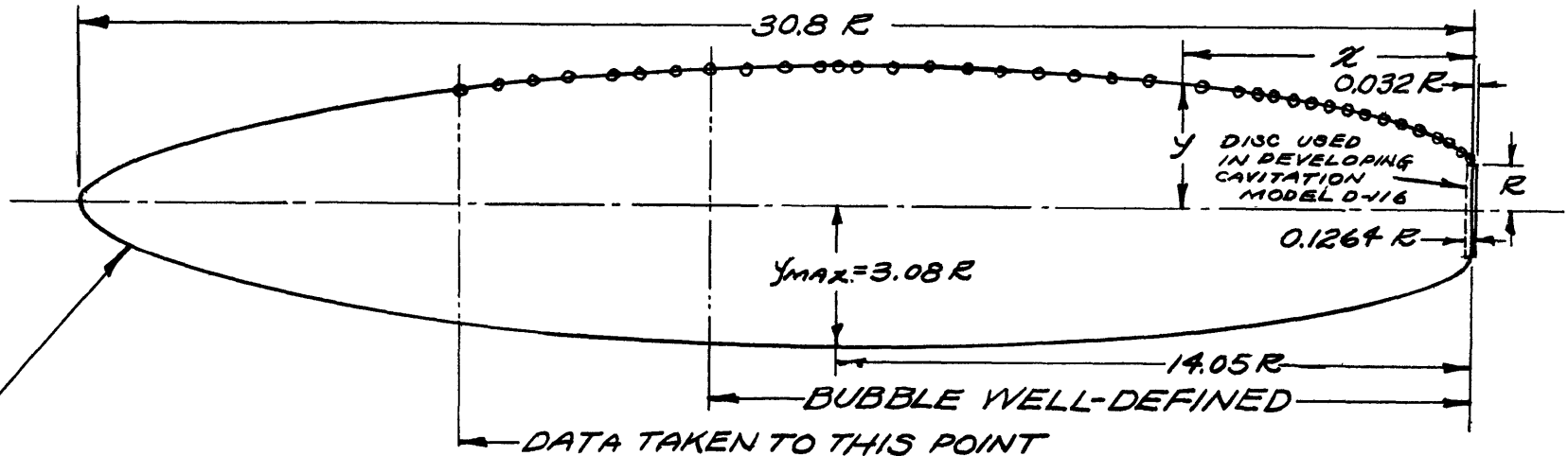


TMB 26206

Figure 4 - Cavitation Model D-116

This model was constructed to the shape of cavitation bubble shown in Figure 3.

DAVID TAYLOR MODEL BASIN



$$v^2 = 1 + 1265(10^{-3})u^{\frac{1}{2}} + 60676(10^{-5})u + 92177(10^{-7})u^2 - 53934(10^{-7})u^3 + 33141(10^{-8})u^4 - 99745(10^{-9})u^5 + 11756(10^{-11})u^6$$

$$u = \frac{r}{R}, v = \frac{y}{R}$$

OFFSETS FOR CAVITATION MODEL D-116					
u	v	u	v	u	v
0.0	1.00	7.0	2.7996	23.0	2.4946
0.1	1.2086	8.0	2.8848	24.0	2.3468
0.2	1.2990	9.0	2.9527	25.0	2.1758
0.3	1.3695	10.0	3.0051	26.0	1.9784
0.4	1.4297	11.0	3.0431	27.0	1.7506
0.5	1.4831	12.0	3.0679	28.0	1.4842
0.6	1.5317	13.0	3.0801	29.0	1.1656
0.7	1.5767	14.0	3.0801	30.0	0.7541
0.8	1.6187	15.0	3.0683	30.1	0.7026
0.9	1.6583	16.0	3.0445	30.2	0.6480
1.0	1.6959	17.0	3.0086	30.3	0.5893
2.0	2.0003	18.0	2.9601	30.4	0.5252
3.0	2.2301	19.0	2.8981	30.5	0.4546
4.0	2.4155	20.0	2.8219	30.6	0.3691
5.0	2.5684	21.0	2.7303	30.7	0.2620
6.0	2.6951	22.0	2.6217	30.8	0.00

FIGURE 5
COORDINATES OF
CAVITATION MODEL
D-116

AUGUST 1947

CONFIDENTIAL

DAVID TAYLOR MODEL BASIN

AUGUST 1947

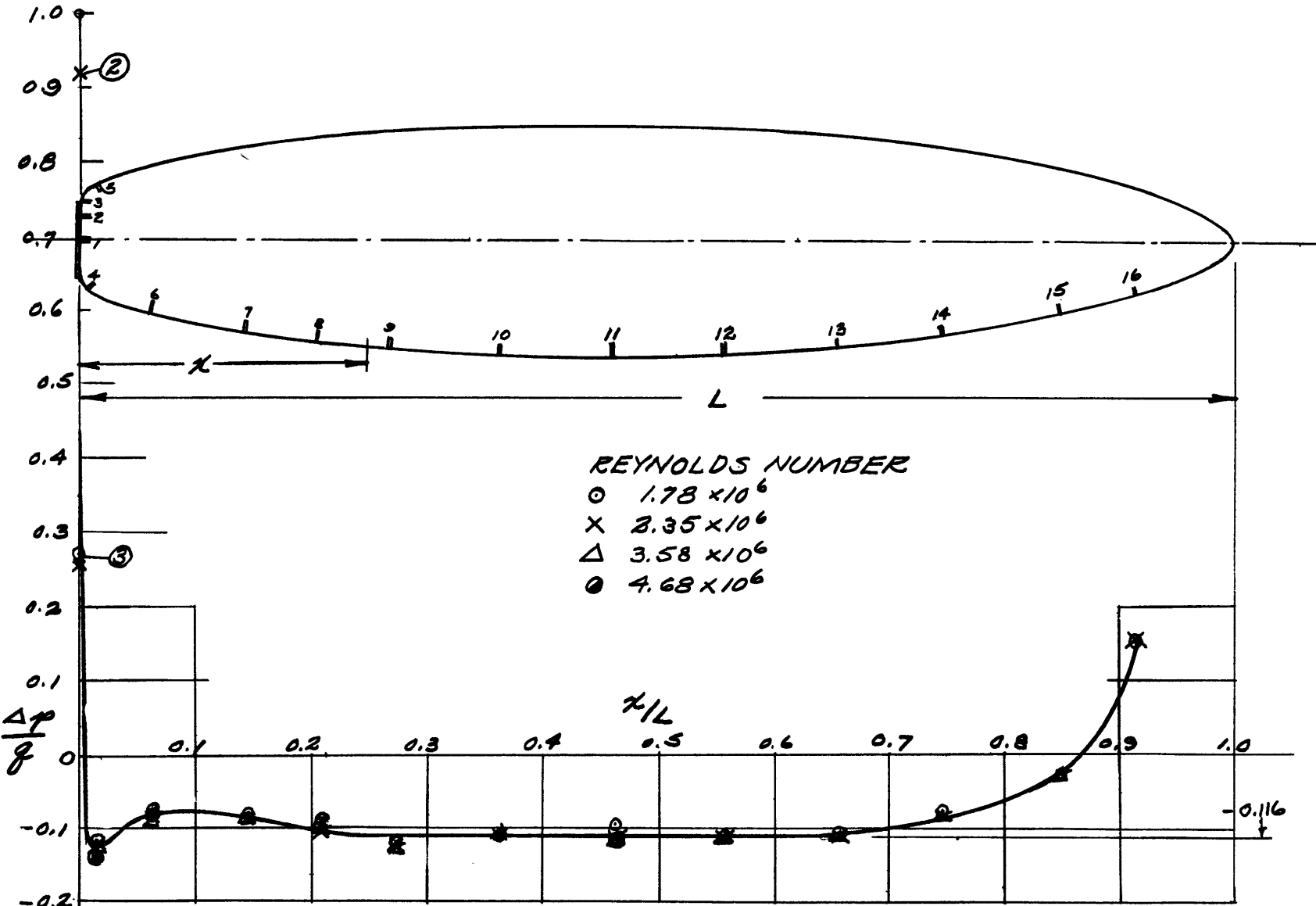


FIGURE 6 - PRESSURE DISTRIBUTION ON CAVITATION MODEL D-116

CONFIDENTIAL



1
1

